Toxicology Research

PAPER

View Article Online
View Journal | View Issue

Cite this: *Toxicol. Res.*, 2019, **8**, 361

Lactobacillus rhamnosus GG reverses mortality of neonatal mice against *Salmonella* challenge

Aman Kumar Naik,[a] Uday Pandey,[a] Raktim Mukherjee,[a] Sohini Mukhopadhyay,[a] Subhayan Chakraborty,[b] Arindam Ghosh[b] and Palok Aich *[a]

Received 8th January 2019,
Accepted 30th January 2019

DOI: 10.1039/c9tx00006b

rsc.li/toxicology-research

Pathogenic infection is one of the major causes of death in newborns. Antibiotic based therapies are still the major mode of treatment for infection. Increased usage of antibiotics leads to selective evolution of microorganisms and causes diseases in adulthood. Attempts to develop alternatives to antibiotics did not yield much success. A recent viable trend is to identify novel probiotics that could alleviate problems associated with over usage of antibiotics. We screened three different *Lactobacillus* species to establish their efficacy in neonates in protecting against *Salmonella* challenge. The methodologies employed are metagenomics, metabonomics, transcriptional profiling, molecular assays and behavioral studies. Among the three probiotics used, only *Lactobacillus rhamnosus* GG (LGG) treatment of the neonates resulted in rescuing of 80% of the *Salmonella*-infected mice. We have shown that LGG (MTCC #1408) can prevent *Salmonella* mediated infection in neonates. In the current report, results from histopathology, gene expression, neutrophil infiltration, metabolite and metataxonomic profiling, and protein level data suggested that LGG treatment of the neonates enhanced anti-inflammatory cytokine expression and increased the gut barrier function. The current report establishes the potential use of LGG in clinical intervention of infectious diseases.

Introduction

In 2010, 7.6 million children under 5 years of age died globally, out of which 64%, *i.e.* about 4.9 million, died of infections such as pneumonia, sepsis, meningitis, typhoid and diarrhea. In India alone, 32% of about 1.7 million children died because of infectious disease[1] and 93 million *Salmonella* infections happen globally every year.[2] *Salmonella enterica* serovar *typhimurium* (ST), a Gram-negative bacterium, is one of the leading causes of gastroenteritis.[3] Gastroenteritis, known as infectious diarrhea, involves inflammation of the gut and severe diarrhea. Recent studies revealed that inflammation in the gut could give a nutritional advantage to *Salmonella* growth by increasing the availability of ethanolamine to provide a competitive advantage to *Salmonella* over other commensals.[4] Reactive oxygen species from an inflamed gut reacts with luminal thiosulphate to produce tetrathionate which acts as a respiratory electron acceptor for *Salmonella*. This respiratory advantage helps *Salmonella* to proliferate in the gut.[5] Inflammatory response helps in colonization of *Salmonella* by disrupting the stable gut microbiota.[6,7] Studies with IL10 knockout mice exhibited more aggressive pathogenesis to *S. typhimurium* infection, supporting the fact that hyper-inflammation assists *Salmonella* in colonization.[7] This result establishes anti-inflammatory immune modulation as a potential therapy for the treatment of *Salmonella* mediated pathogenesis.

Probiotics are commensal microorganisms which exert several physiologically beneficial effects on the host including anti-inflammatory responses. *Lactobacillus rhamnosus* strain GG (LGG) was initially isolated from newborn babies by Gorbach and Goldin.[8] Recently LGG was used as a preventive intervention for the DSS induced inflammatory bowel disease (IBD) model in mice.[8] Studies performed by Yan *et al.* revealed that LGG administration caused anti-inflammatory modulation to suppress the IBD.[8] The study by Yan *et al.* further revealed that LGG treatment increased gut epithelial barrier functioning by decreasing gut permeability.[8] LGG administration has been shown to increase IL-10 secretion in humans.[9] Results from the studies indicated that LGG may be one the best candidates for the treatment of *Salmonella*-mediated pathogenesis.

In the current study we have used a neonate mouse model for ST challenge studies to establish the efficacy of LGG. ST usually causes gastroenteritis in humans and cattle but not in

[a]*School of Biological Sciences, National Institute of Science Education and Research (NISER), HBNI, P.O. – Bhimpur-Padanpur, Jatni – 752050, Dist. – Khurdha, Odisha, India. E-mail: palok.aich@niser.ac.in; Fax: +916742494004; Tel: +916742494133*
[b]*School of Chemical Sciences, National Institute of Science Education and Research (NISER), HBNI, P.O. – Bhimpur-Padanpur, Jatni – 752050, Dist. – Khurdha, Odisha, India*

adult mice. Mice are resistant to *Salmonella* mediated gastroenteritis. In mice, only mild inflammation is observed following *Salmonella* infection.[10,11] Streptomycin treated adult mice, however, are an established murine model to study *Salmonella* mediated gastroenteritis.[12] But a streptomycin treated mouse model is not suitable for gut microbiota study as streptomycin treatment disrupts the gut microbiota. It has been recently shown that intestinal microbiota play critical roles in regulating infectivity and transmissivity of *Salmonella* infection.[13]

Administration of *Salmonella* to the neonates has been shown recently to cause full-scale pathogenesis and gastroenteritis.[14] It is, therefore, of higher interest to study *Salmonella* pathogenesis and to develop a plausible treatment protocol in neonate mice. For this purpose, LGG treatment before a challenge with *Salmonella* in neonates is a potential way of preventing *Salmonella* infection by means of activating anti-inflammatory pathways. The current study clearly showed that LGG treatment, which began a day prior to *Salmonella* challenge on day 5, and continued for the rest of the study period could alleviate *Salmonella* infection by (a) reducing mortality, (b) increasing the molecular expression of genes associated with the host gut barrier and anti-inflammatory responses, (c) increasing the neuro-muscular strength of the mice and (d) altering gut microbiota. Because of practical difficulties, detailed cellular level validation to establish the exact mechanism of LGG action could not be reported in the current study. We have, however, correlated the tissue level immune response with that of the systemic response in the host by analysing metabolite profiling.

Experimental

Bacteria culture

Lactobacillus acidophilus (MTCC #10307), *Lactobacillus rhamnosus* GG (MTCC # 1408), and *Salmonella enterica* serovar *typhimurium* (MTCC #3232) were obtained from the Microbial Type Culture Collection and (MTCC). *Lactobacillus delbrueckii* subsp. *Bulgaricus* (strain DWT1) was received as a gift from Daflorn Private Limited, a Bulgarian probiotic company. All *Lactobacillus* strains were cultured in De Man, Rogosa and Sharpe agar. *Salmonella* was cultured in nutrient broth. Bismuth sulfite agar was used as a differential medium for *Salmonella*.

Animal experiments

BALB/c mice were used for the experiments. All animals were acquired from the NISER Animal Facility and all the procedures used for animal studies were approved by the Institute Animal Ethics Committee (IAEC), NISER that is approved by the Committee for the Purpose of Control and Supervision of Experiments on Animals (CPCSEA) of the Government of India and co-housed in a specific pathogen free (SPF) facility. Male and female 6–8 week-old mice were kept for breeding in a cage in a 1 : 2 ratio. Neonates (irrespective of any gender bias as gender bias may not be an important factor at this age unlike adult mice) were challenged with the required amount of *Salmonella*. The dosage of the *Salmonella* challenge was determined from a dose titration between 10^3 CFU per mouse and 10^8 CFU per mouse and the challenge dose was selected as 10^6 CFU per mouse based on survival data as detailed in the Results section. *Salmonella* was gavaged once orally into mice on day 5 post birth. Probiotics were administered daily from postnatal day 4 (a day prior to *Salmonella* challenge) using a 24 gauze feeding tube.

Infection severity index scoring

The scoring method was adapted from Kim *et al.*[15] The scoring was double-blinded to both scorers and to the introducer.

Cytokine analysis

Colon tissues were collected on day 8 post-infection from treated and un-treated mice. The colon was washed with 1× PBS and visible fat tissues were removed. The samples were churned in lysis buffer (Tris-hydrochloric acid, sodium chloride, and Triton X-100 in distilled water) containing a 1× protease inhibitor cocktail (PIC) (Himedia, India). The mixture was centrifuged and the supernatant was collected and used for further analysis. The protein level abundance of genes for *TNF*, *IL-10*, and *IL-4* was measured by ELISA. An ELISA assay kit was purchased from BD Biosciences, USA and the assay was performed using the manufacturer's protocol. For absorbance reading, Multiskan GO instrument (Thermo Fisher Scientific, USA) was used. For normalization, protein concentration was measured using the Bradford assay (BD Biosciences, USA). The protocol was adopted from an earlier report as described in Kim *et al*.[15]

RNA extraction and cDNA preparation

Colonic tissues were stored in RNALater (Sigma Aldrich, USA). The tissues were churned using RLT buffer and further RNA extraction was done using an RNeasy Mini Kit (Qiagen, Germany) as described in the manufacturer's protocol. cDNA was synthesized from the RNA using an AffinityScript Herc. II RT-PCR kit (Agilent Technologies, USA).

Primer designing

Primers for genes were designed using Primer BLAST.[16] The species-specific primer was designed against the 16s rRNA gene. The 16s rRNA sequence of the species of interest was taken from NCBI Nucleotide Database.[17] Then it was aligned with the 16s rRNA database in BLAST.[18] The top 50 hits were taken and aligned in MUSCLE.[19] The unique sequence of interest was searched for. The 3′-OH was fixed as base G or C in the sequence of interest and the base was extended towards the 5′ end until the melting temperature (T_m) of 55 °C is reached. The species specificity of the primers was checked using blast.

Table 1 Fold change values of significantly and differentially expressed genes as reported for treatment with LGG, challenge with ST and treatment with LGG following challenge with ST. Fold change values are computed with respect to time matched untreated (control) neonatal mice

	Fold change values (±SD)			*p*-Values		
	LGG	ST	LGGST	LGGST *vs.* ST	LGGST *vs.* LGG	ST-LGG
NOS2	4.7 ± 2.72	226.46 ± 70.7	13.5 ± 1.67	0.0004	ns	0.0003
IL1B	18.24 ± 3.09	100.46 ± 8.06	3.72 ± 2.73	<0.0001	0.0184	<0.0001
T-bet	0.74 ± 0.33	1.73 ± 0.37	0.79 ± 0.27	0.0144	ns	0.0102
TLR4	0.04 ± 0.01	16.48 ± 6.27	0.03 ± 0.03	0.0009	ns	0.0009
IL10	5.61 ± 0.16	3.55 ± 0.17	7.22 ± 0.64	<0.0001	0.0019	0.0004
GATA3	1.71 ± 0.22	0.55 ± 0.06	1.04 ± 0.18	0.0159	0.0023	<0.0001

qRT PCR

The qRT PCR was done using SYBR green chemistry using a GoTaq qPCR Kit (Promega, USA). The final volume of the reaction mixture was 25 μl per well. The relative gene expression values were calculated using the ΔΔCt method. The standard curve to determine *Salmonella* CFU count in the fecal sample was evaluated by spiking known CFU of ST in the fecal samples from un-infected (control) mice; spiking of ST was increased from 10^3 CFU per mouse up to 10^8 CFU per mouse with multiples of 10 CFU for every interval. *Salmonella* chromosomal DNA was isolated from spiked fecal samples (n = 3) and copy number was determined by PCR using the *Salmonella* specific primer. qRT-PCR was used to determine the fold change of select genes by comparing the expression of genes for the treated and un-treated samples. The primer sequences used for various genes are enlisted in Table 2.

MPO activity assay

The myeloperoxidase (MPO) assay is done to evaluate neutrophil infiltration. MPO is a peroxidase enzyme that is expressed abundantly in neutrophil granulocytes. It is a lysosomal protein stored in the azurophilic granules of the neutrophil. Myeloperoxidase contains a heme pigment which causes its green color in secretions rich in neutrophils, such as pus and some forms of mucus. Myeloperoxidase catalyzes the production of hypochlorous acid (HClO) from hydrogen peroxide (H_2O_2) and the chloride anion (Cl-, or the equivalent from a non-chlorine halide). The MPO assay was done as described elsewhere.[15] 50 mM solution of potassium phosphate buffer was prepared by adding solution B (K_2HPO_4, 8.7 g in 1 L of dH_2O) to solution A (KH_2PO_4, 6.8 g in 1 L of dH_2O) until a pH of 6.0 was achieved. 25 mg colonic tissue was churned in 2 ml of HTAB buffer (5 g HTAB in 1 L of potassium phosphate buffer) and the supernatant was collected following centrifugation. *o*-Dianisidine dihydrochloride (*o*-dianisidine) solution was prepared by mixing 16.7 mg of *o*-dianisidine dihydrochloride (Himedia, India), 90 mL of dH_2O, and 10 mL of potassium phosphate buffer. 50 μL of diluted H_2O_2 (4 μL of 30% H_2O_2 diluted in 96 μL of dH_2O) was added to the *o*-dianisidine solution. 50 μL of the collected supernatant was taken in triplicate for each biological sample and replicated. 200 μL of *o*-dianisidine solution was added to each well and the absorbance at 450 nm was measured. MPO unit per mg of protein was calculated using following formula.

$$[\Delta A(t_2 - t_1)]/[\Delta_{\min} \times (1.13 \times 10^{-2})]/0.625.$$

Table 2 List of forward (_F) and reverse (_R) primers for genes used in this report for qPCR studies

Gene	Primer pair
ST_F	5′-AGGCGTGGCTTCCGGACG-3′
ST_R	5′-GAAGGCACCAATCCATCTCTGGATTC-3′
T-bet_F	5′-AGGATGTTTGTGGATGTGGT-3′
T-bet_R	5′-ACATATAAGCGGTTCCCTGG-3′
GATA3_F	5′-CTCCTTGCTACTCAGGTGAT-3′
GATA3_R	5′-GAGAGAGGAATCCGAGTGTG-3′
Muc2_F	5′-GTGATTGTGTTTCAGGCTCC-3′
Muc2_R	5′-GTACATGGCAAAAGTCCCAC-3′
cldn-3_F	5′-AAGATCCTCTATTCTGCGCC-3′
cldn-3_R	5′-TTCATCGACTGCTGGTAGTG-3′
Il-1B_F	5′-GCCACCTTTTGACAGTGATG-3′
Il-1B_R	5′-GCCTGAAGCTCTTGTTGATG-3′
Ocln_F	5′-GTTGAACTGTGGATTGGCAG-3′
Ocln_R	5′-AAGATAAGCGAACCTTGGCG-3′
Cldn1_F	5′-TGCCCCAGTGGAAGATTTACT-3′
Cldn1_R	5′-CTTTGCGAAACGCAGGACAT-3′
Il-10_F	5′-TGGGAGGGGTTCTTCCTTGG-3′
Il-10_R	5′-GGGAACCCTCTGAGCTGCTG-3′
Tlr4_F	5′-CGCTGCCACCAGTTACAGAT-3′
Tlr4_R	5′-AGGAACTACCTCTATGCAGGGAT-3′
Nos2_F	5′-GCAACTACTGCTGGTGGTGACAG-3′
Nos2_R	5′-GGAAGTGAAGCGTTTCGGGATCTG-3′

Details of the genes are described in the main text.

Histology

Tissue samples from the ileum, colon, liver and spleen were collected and stored in 4% paraformaldehyde solution for H&E staining. Tissues were processed for paraffin embedding, and multiple 5-micron sections were prepared. For staining, slides were de-paraffinized by dipping in xylene and hydrated with deionized water followed by hematoxylin (Sigma Aldrich, USA) and eosin staining (Himedia, India). For better visibility of the nucleus, bluing solution (1% $MgCl_2$ and 0.07% sodium bicarbonate) was used. Slides were thoroughly washed in water, dehydrated through sequential alcohol grading, then cleared in xylene and mounted with permanent mounting media (Vector Labs, USA). Stained slides were observed under a Leica DM500 light microscope, and representative images were taken at 4×, 10× and 40× magnifications.

Histopathology scoring

The following method was used for scoring histological samples. All the slides were given ID and were distributed to the lab members (they were blind to the sample types); the distributor of the slides was also blind to the sample types. The median score from the different representatives was taken. The scoring method was adapted as described before.[20]

Ambulation test

The ambulation test is designed to check the balance while walking. Pups were placed on a white rough surface where they were visible from the side as well as the top. Gently pups were prodded so that they will be induced to walk. The scoring method was adapted from Feather-Schussler *et al.*[21]

Grip strength test

The pup of interest was placed on a wire mesh. For approximately 5 s the pup was allowed to adjust to the environment. The mesh was slowly rotated until it attained 180 degrees. The approximate angle at which the pups got detached from the mesh was recorded. If mice remained attached until 180 degrees, then the hanging impulse was calculated by multiplying the time for which a mouse stayed attached (in seconds) with the weight of the mouse (in grams).[21]

Grasping reflex

The mouse was held by its neck like when it is carried by the dam. Each paw of the mouse was stroked with a bluntly rounded plastic card. The number of paws with which it grasped the card was measured.[21]

It is known that *Salmonella* infection leads to disbalance or loss of strength for gripping and grasping. The tests for ambulation, grip strength and grasping were designed to establish whether LGG could prevent such behaviour following *Salmonella* challenge.

Sample preparation for metabolomics

Functional characterization of serum metabolites is performed to see whether the immune alterations observed in the gut following *Salmonella* challenge with or without LGG can affect the metabolic profile at the systemic level of the host. For the serum extraction, the blood of the neonates was collected using the cardiac puncture method and serum was extracted by centrifuging blood at 1300*g* for 10 min. Abundant proteins in the serum were removed by passing it through pre-rinsed (7 times washed) Amicon Ultra-2 ml 3000 MWCO filters (Merck, Millipore, USA) at 4 °C and 12 000*g* centrifugation. A total of 700 μL of sample containing D_2O, pH maintenance buffer and DSS as the reference sample was taken in 5 mm Shigemi tubes.

NMR data acquisition

All experiments were performed at 298 K on a Bruker 9.4T (400 MHz) AVANCE-III Nanobay liquid-state NMR spectrometer equipped with a 5 mm broadband (BBO) probe. A presaturation technique was used with a moderate relaxation delay of 5 seconds to ensure complete water saturation. Offset optimization was performed using real-time 'gs' mode for each sample. Topspin 2.1 was used to record and process the acquired spectra.

Metabolomic analysis of NMR data

The NMR data were analyzed in ChenomX (Canada) which derived the concentrations of metabolites in the serum using a Bayesian approach. The raw spectrum was phase and baseline corrected. Then through the profiler different concentrations of metabolites were obtained. The concentration file was then analyzed in Metaboanalyst.[22,23] The sample was log transformed for normalization. Fold change analysis was performed for each of the samples in comparison with the untreated control. 2 log fold up- or down-regulated metabolites were considered significant. Then PCA was performed to see the differential clustering of samples and a 2D PCA plot was generated. A heat map was generated using Ward clustering algorithm where Euclidean distance measurement was used. Then pathway analysis was performed to obtain the associated pathways. Fisher's exact test was used to do over-representative analysis and out-degree centrality algorithm was used to do pathway topology analysis. All the analyses performed related to metabolomics were done in Metaboanalyst.

Cecal DNA extraction

A cecal sample was collected from day 8 post-infected neonate mice and stored at −80 °C. DNA from the cecal sample was isolated using a QIAamp DNA Stool Mini Kit (Qiagen, Germany). The same method was followed as that described in the manufacturer's protocol.

16s rRNA sequencing (V3–V4 metagenomics)

V3–V4 regions of 16S rRNA gene from cecal DNA samples were amplified using the primer pair V3F: 5′-CCTACGGG NBGCASCAG-3′ and V4R: 5′-GACTACNVGGGTATCTAATCC-3′. Then amplicons were sequenced using paired end (250bpX2) sequencing in an Illumina Miseq platform and sequencing depths of 393 503 ± 151 816 reads (mean ± SD) were generated. Subsequently, a FASTQ quality check was performed where the base quality, base composition and GC content were checked. For all the samples more than 90% of the sequences were having Phred quality scores of more than 30. For all the samples GC content was nearly 30–60%. Conserved regions from the paired end reads were removed. Using FLASH program, a consensus V3–V4 region sequence was constructed after trimming the unwanted sequences from the original paired-end data. Pre-processed reads from all the samples were pooled and clustered into Operational Taxonomic Units (OTUs) using the *de novo* clustering method based on their sequence similarity using UCLUST program. QIIME was used for OTU generation and taxonomic mapping.[24] A representative sequence was identified for each OTU and aligned against a Greengenes core set of sequences using PyNAST program.[25,26] Furthermore, we aligned these representative sequences against reference chimeric data sets. Then taxo-

nomic classification was performed using the RDP classifier against SILVA OTUs database.

Microbiota compositional profiling and analysis

The biome file containing all phylogenetic information was used for further analysis in MicrobiomeAnalyst.[27] The features were filtered for minimum counts of 2 and 20% prevalence. The lowest variance *i.e.* 10% was also filtered. The data were scaled using total sum scaling algorithm. A stacked bar plot with percentage abundance was generated. A heat map for phylum level data was generated using Ward clustering algorithm and Euclidean distance measurement. Chao1 diversity measure was used to calculate alpha diversity of each sample. The beta diversity measurement was performed using an ordination based method, principal coordinates analysis, where the distance method was the Bray-Curtis index and the statistical method used was permutational MANOVA (PERMANOVA).

Microbiota functional profiling and analysis

For microbiota functional profiling, closed reference OTU picking was performed and taxonomy based mapping was done using Greengenes taxa 13.8 database. After obtaining the biome file it was further processed in PICRUST for metagenomic prediction.[28] The predicted metagenome was used to obtain the KEGG orthologue functional category. The resulting biome file was analyzed in MicrobiomeAnalyst for further clustering and diversity analysis.

Statistical analysis

All the graphs were plotted using GraphPad Prism 7.0a. The statistical package in Prism was used for statistical analysis of the data to perform the *t*-test (to compare any 2 data sets) or ANOVA (to compare more than two datasets) as described in the text.

Results

LGG treatment rescues *Salmonella*-infected neonates and reduces pathogenesis

Doses of 1×10^7 CFU per mouse for each of *Lactobacillus acidophilus* (LA) and *Lactobacillus delbrueckii* subsp. *Bulgaricus* DWT1 (LDB) were chosen for treatment as described elsewhere.[8,20] Treatment of BALB/c mice with LA and LDB showed nearly 50% lethality in neonates. A daily dose of LA of 1×10^7 CFU mL^{-1} and LDB of 1×10^7 CFU mL^{-1} could not rescue *Salmonella* infected neonates. These results suggested that LA and LDB treatment was not potent enough to alleviate *Salmonella* infection and, moreover, LA and LDB were lethal to half of the animals. Higher doses of these probiotics were toxic to neonates (Fig. 1A). Treatment with LGG, in contrast, could protect the neonates from *Salmonella* infection (Fig. 1B). *Salmonella* infection in neonates was standardized based on the survivability data of different *Salmonella* doses as described in the Materials and methods section. The percentage of mouse surviving against days post infection at different dosages of *Salmonella* was evaluated for *Salmonella* challenge dose titration between 10^3 CFU per mouse and 10^8 CFU per mouse. Challenge doses from 10^3–10^5 CFU per mouse took 15–20 days to set the infection, while doses above 10^7 CFU per mouse set the infection in 3 days in neonate mice. Results with a challenge dose of 10^6 CFU per mouse took around 8–10 days to set *Salmonella* infection. We selected the *Salmonella* challenge dose of 10^6 CFU per mouse to have sufficient time to study the effects of challenge on neonates as well as give enough room to study the effects of probiotic treatment. The current report revealed that around 80% of the neonates have been rescued from *Salmonella* infection following treatment with LGG (Fig. 1B). The data shown are the average of 15 neonates taken randomly from different littermates to minimize the litter biases. The dose of 1×10^7 CFU mL^{-1} of LGG was chosen based on previous studies.[8] No deaths were observed when only LGG was administered orally. Three out of 15 *Salmonella* challenged neonate mice died following treatment with LGG while all *Salmonella* challenged pups died without LGG treatment by day 11 post challenge. Since the studies involved neonates from a very early age (day 3 onwards), methodologies to distinguish the pups based on gender are not very reliable and since the studies were completed before they reached the age of weaning (3 weeks), we did not attempt to separate the pups in the groups into males and females, because the effects would have been minimal based on gender difference for this infection-protection study.

Scoring for infection severity (see the Materials and methods section) was done for LGG treated and un-treated neonates in the ileum, colon, liver and spleen. *Salmonella*-infected mice showed signs of diarrhea on 4–6 days post infection. But mice treated with LGG delayed the onset of diarrhea on days 13–16 post-infection. *Salmonella*-infected mice showed rectal bleeding, rectal prolapse and also blood in feces. The LGG treated *Salmonella* challenged mice did not show any of those symptoms (Fig. 1C).

It has been reported previously that *Salmonella* infiltrates the gut epithelium that leads to infection in multiple organs.[14] Finally, multiple organ failures led to death of the neonates. It is, therefore, important to regulate the systemic inflammation for controlling the pathogenesis. Treatment with LGG showed a significant reduction in the *Salmonella* CFU count in the total gut tissue, liver and spleen ($P < 0.01$) (Fig. 1D–F). This observation suggested a systemic effect of LGG treatment. In the cecal content, *Salmonella* count was also significantly low in the LGG treated sample ($P < 0.05$) (Fig. 1D). In neonate mice, the average *Salmonella* count found in the gut following *Salmonella* challenge was similar to the challenge dose *i.e.* 10^6 CFU per mouse. Following treatment with LGG in *Salmonella* challenged mice, the count reduced to 10^4 CFU per mouse.

LGG treatment reduces inflammation in *Salmonella*-infected neonates

The ileum and colon of the *Salmonella*-infected mice showed severe immune cell infiltration (Fig. 2). Fig. 2 presents histology images and scores for the ileum, colon, liver and spleen

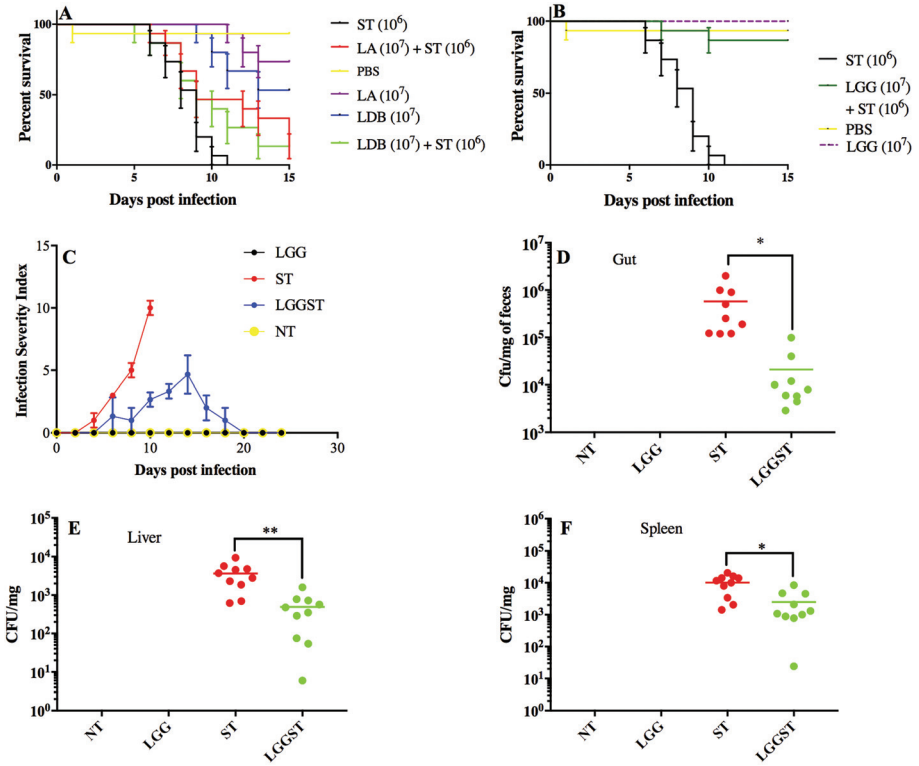

Fig. 1 LGG treatment rescues neonates from *Salmonella* challenge. A Kaplan–Meier plot of survivability of neonates (A, B). A: Neonates challenged with *Salmonella* at 10^6 CFU per mouse showing 50% mortality on day 8 post infection. *Lactobacillus acidophilus* (LA) at 10^7 CFU per mouse dosage was toxic to neonates. *Lactobacillus delbrueckii* subspecies *bulgaricus* (LDB) at 10^7 CFU per mouse was also toxic to neonates. All mice (n = 15) that were treated with either LA or LDB on day 4 and continued until the end died by day 15 following *Salmonella* (10^7 CFU per mouse) infection on day 5. B: *Lactobacillus rhamnosus* GG (LGG) at a dosage of 10^7 CFU per mouse could protect 80% of mice beyond day 15. C: Infection severity index calculated for neonates in each interval post infection and treatment. D: ST count using the culture method in caecal matter of neonates on day 8 pi (P value <0.05). E: ST count using the culture method in the liver of neonates on day 8 post infection (pi) (P value <0.01). F: ST count using the culture method in the spleen on day 8 pi (P value <0.05). Unpaired t-test was performed to calculate the significant values for (D, E, and F). Each group consisted of n = 15 neonatal mice.

of untreated (NT), LGG treated, ST challenged and LGG treated but ST challenged mice. Results indicated severe villi atrophy (Fig. 2). The *Salmonella* challenged pups had a smaller length of villi left compared to the uninfected pups. The LGG treated sections showed less, or in some cases, no immune cell infiltration and also the ileum and colon were less damaged. The goblet cells were fully destroyed in *Salmonella*-infected mice (Fig. 2). The *Salmonella*-infected mice also displayed severe liver damage compared to LGG treated mice (Fig. 2). In the spleen of *Salmonella*-infected mice, lymphoid sheath immune cell clusters were observed whereas LGG treatment revealed very little sheath development (Fig. 2). Damage to the liver and spleen, as determined from the histology scores, confirmed the presence of *Salmonella* and exhibited signs of systemic inflammation. In all cases, histopathology scores from the LGG treated group were significantly less than the histopathology scores obtained from the un-treated group ($P < 0.0001$) (Fig. 2A–D).

Current results revealed that TNFα, a proinflammatory marker, was significantly high following *Salmonella* challenge, while it came back to normal levels in mice that were treated with LGG followed by *Salmonella* challenge (Fig. 3A). In the current study, we also observed that both MPO activity (Fig. 3B) and IL-8 gene expression (Table 1) are higher in *Salmonella*-infected mice. It was reported that iNOS expression increases in the presence of *Salmonella* infection because of macrophage infiltration.[29] In the current study, we established that the expression of iNOS gene was significantly low in (a) LGG treated control mice and (b) *Salmonella* challenged but LGG treated neonates (Table 1). Current results further revealed a higher expression level of IL-1B gene, an inflammatory cytokine, following challenge with *Salmonella*. The expression of IL-1B is significantly reduced following LGG treatment in *Salmonella* challenged mice (Table 1). The anti-inflammatory cytokine IL-4 was also seen to be highly expressed in LGG treated pups (Fig. 3C). We also showed that IL10 is significantly overexpressed at mRNA and protein levels in LGG treated mice than *Salmonella*-infected mice (Table 1, Fig. 3D). It is known that the SP-1 gene cluster of *Salmonella* activates IL-1B through inflammasome activation.[30] High GATA3 expression again indicates a Th2 modulation by LGG treatment in the gut. *Salmonella* mediated host response required both TLR4 and its adapter, MyD88. Mice lacking functional TLR4 showed more susceptibility to *Salmonella*

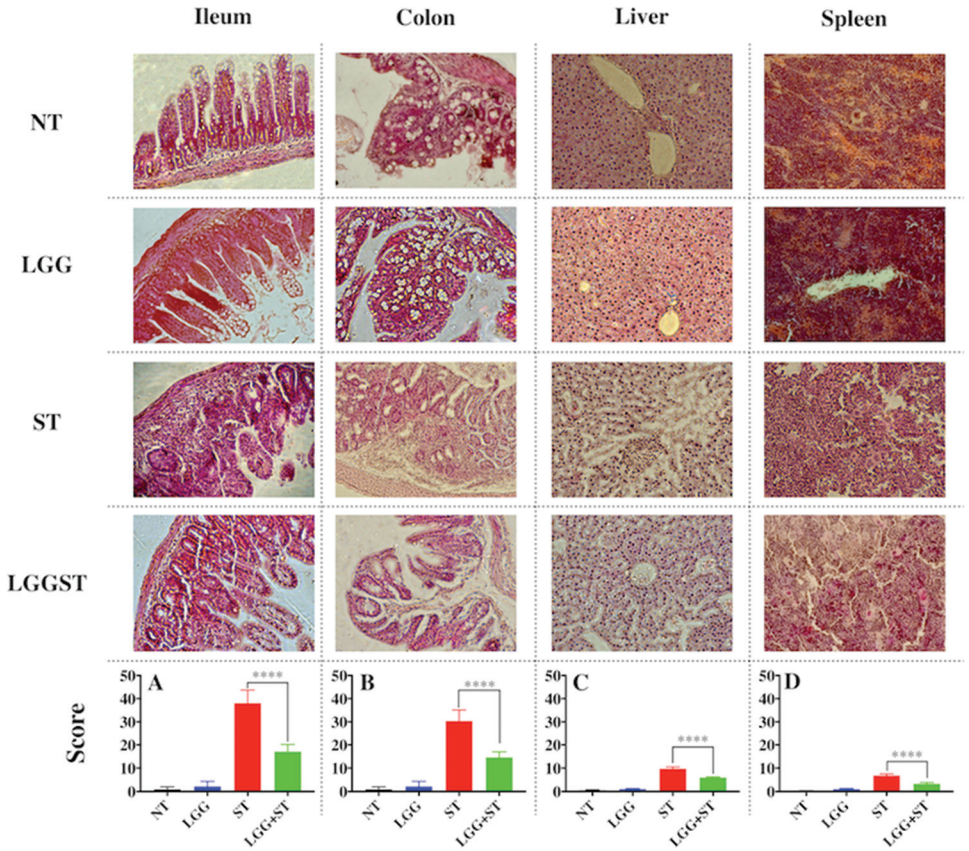

Fig. 2 LGG treatment decreases *Salmonella* mediated pathology of the gut, liver and spleen. The figure presents the eosin and hematoxylin staining of the corresponding samples. One of the representative images of each sample *i.e.* time matched (day 8) untreated (NT), day 8 post infected *Salmonella* (ST), day 8 post-treatment of LGG (LGG), and LGG to *Salmonella* infected (LGG + ST) pups. Histopathology scores of all collective images of the ileum (A), colon (B), liver (C), and spleen (D) (P value <0.001). Unpaired t-test was performed to calculate the significant value in (A)–(D). Histology scores are the average of n = 3 mice per condition.

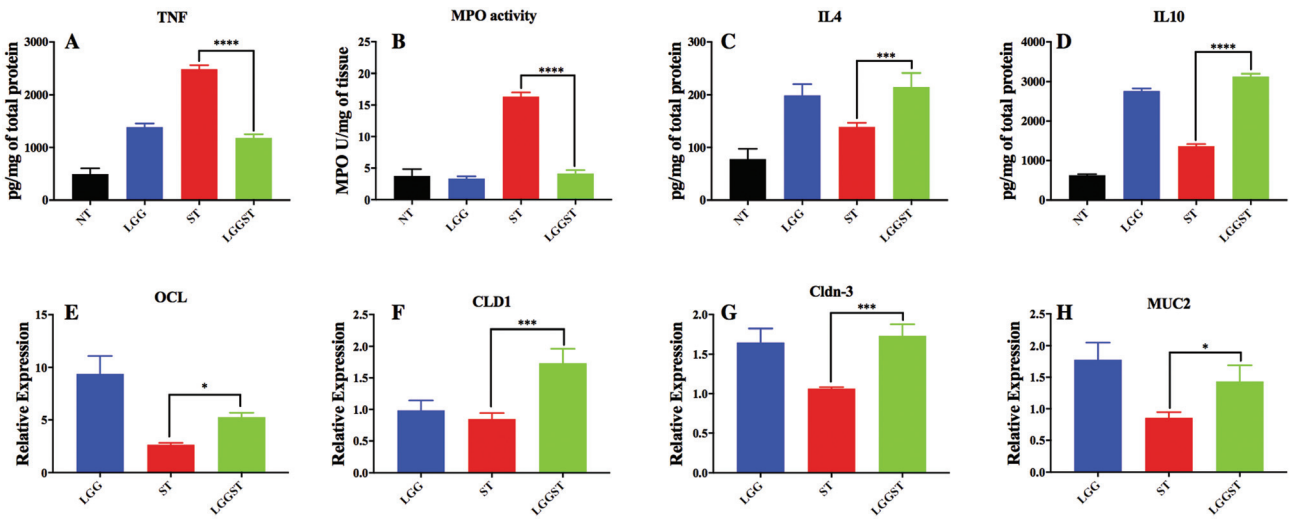

Fig. 3 LGG treatment decreases inflammation and increases gut barrier function and gene expression. A: Cytokine level for TNF in gut tissue (P value <0.001). B: Myeloperoxidase activity in day 8 pi gut tissue (P value <0.001). C: Cytokine level for IL4 in day 8 pi gut tissue (P value <0.001). D: Cytokine level for IL10 in day 8 pi gut tissue (P value <0.001). E: Occludin gene expression level with respect to NT (P value <0.05). F: Claudin1 gene expression level with respect to NT in day 8 pi gut tissue (P value <0.001). G: Claudin3 gene expression level with respect to NT in day 8 pi gut tissue (P value <0.001). H: Mucin2 gene expression level with respect to NT in day 8 pi gut tissue (P value <0.05). Data presented are the average of n = 3 mice per condition.

infection.[31,32] Results from the current report suggested increased expression of TLR4 following challenge with ST in neonates. The reduction in TLR4 expression in ST challenged but LGG treated mice further correlated with the fact that the *Salmonella* count has been reduced (Table 1). In the current study, we found that the expressions of the gut epithelial barrier junction proteins such as Occludin-1, Claudin-1, and Claudin-3 were significantly increased in the LGG treated group compared to the un-treated control group (Fig. 3D, E and F). The Mucin-2 gene expression was also significantly increased in LGG treated mice (Fig. 3G). The results revealed an increase in barrier function or a decrease in gut permeability.

It has been described earlier that ambulation is related to stress and anxiety.[33] The current report revealed that the *Salmonella*-infected mice were having low ambulation scores. This may be because of the defective transition in the limb movement. The effects are found to be reversed following treatment with LGG (Fig. 4A). In the untreated control and LGG treated pups, the grasping reflex test showed that, in most of the cases, the *Salmonella*-infected mice were defective in both of the hind paw reflexes. Conversely, LGG treatment rescued the mice from the hind paw grasping defect (Fig. 4B). Data in Fig. 4C and D revealed that *Salmonella*-infected mice could not show strong grip strength. LGG treatment, however, could rescue the neonates from defective grip strength. *Salmonella*-infected pups were detaching from the mesh at nearly a 100° angle. Untreated control and LGG treated pups were falling at a 180° angle. LGG treated *Salmonella* infected pups showed a reduced angle of inclination at which pups were falling. Hanging impulse was almost zero in the case of *Salmonella*-infected pups. LGG treatment significantly increased the hanging impulse in these pups.

LGG treatment and *Salmonella* infection alters the microbiota of the gut

Treatment with LGG following challenge with *Salmonella* changed both the structure and function of gut microbiota as shown in Fig. 5A and B. Beta diversity graphs (Fig. 5A and B) present different clustering of microbiota in both functional and structural levels. *Salmonella*-infected gut revealed low alpha diversity of gut microbiota (Fig. 5C). LGG treatment, however, showed an increase in the alpha diversity (Fig. 5C). KEGG orthologue based functional classification also differentially clustered different groups suggesting that microbiota are different both structurally and functionally.

Fig. 5D presents phylum level profiling of microbiota for various treatment or challenge conditions. Proteobacteria mainly consist of Gram-negative bacteria. This phylum includes a wide range of pathogens including *Salmonella*. The results explain the pathogenicity of *Salmonella* in infected mice. Thaumarchaeota mainly involves extreme ther-

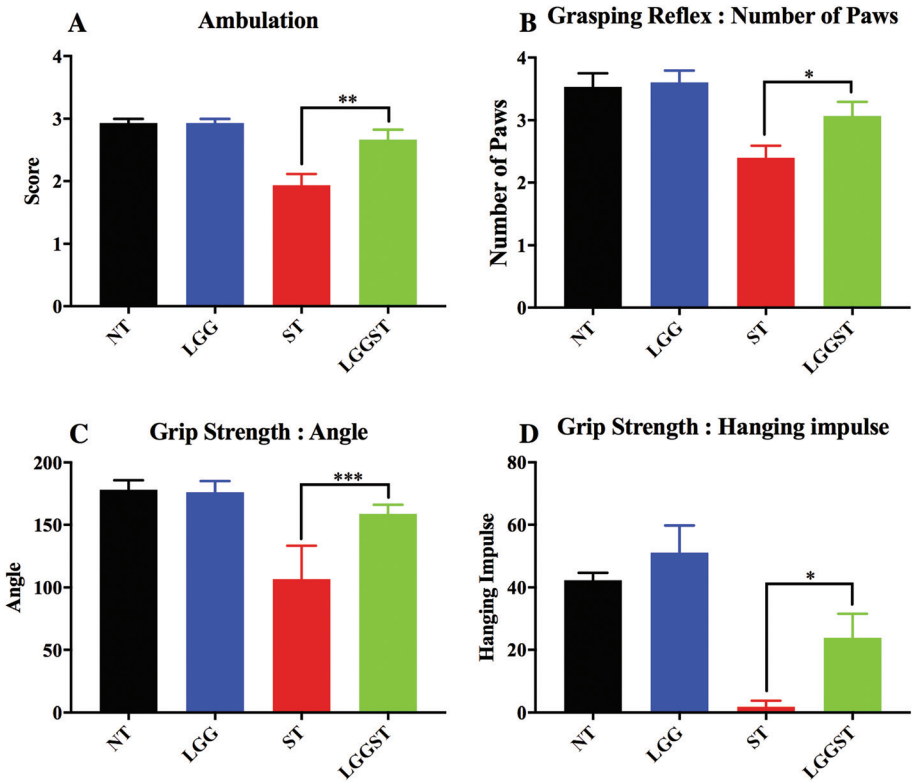

Fig. 4 LGG treatment rescues the neonates from *Salmonella* mediated strength related defects. A: Ambulation test for day 5 pi neonates (P value <0.01). B: Grasping reflex test for day 8 pi neonates (P value <0.05). C: Grip strength test, measurement of detachment angle (P value <0.001). D: Grip strength test, measurement of hanging impulse (P value <0.05). Each experiment was done with n = 5 neonatal mice.

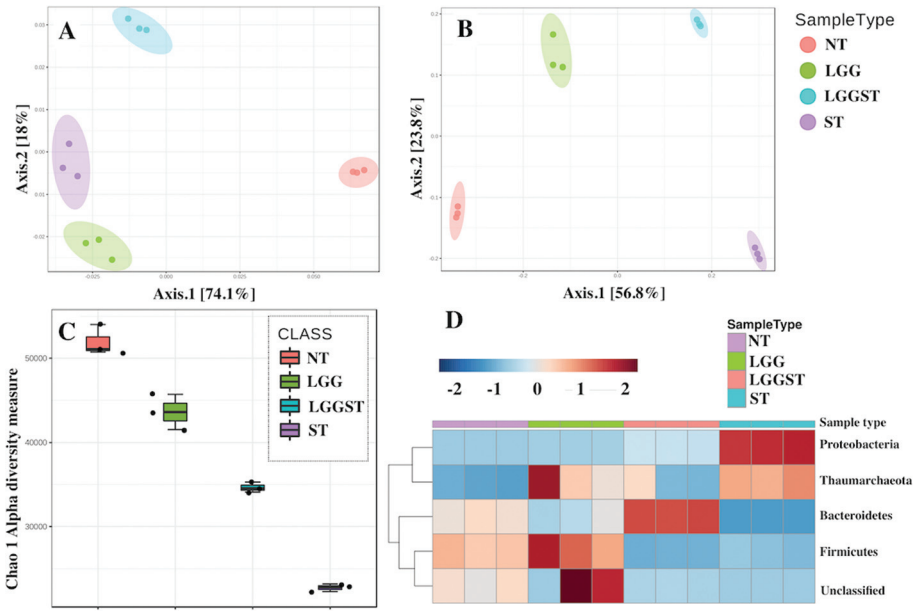

Fig. 5 LGG treatment alters the host microbiota. A: Functional beta diversity plot from PICRUST predicted metagenome for all day 8 pi caecal samples. B: Structural beta diversity plot for day 8 pi caecal samples from 16s rRNA marker based analysis. C: Chao1 alpha diversity measurement for day 8 pi caecal samples. D: Heat map presenting the change in phylum level in the day 8 pi caecal sample. Metagenomic analysis data are presented as the average of n = 5 neonatal mice per condition.

mophiles, and thus does not have a known function in explaining disease severity. The phylum, Firmicutes, mainly consists of Gram-positive bacteria. Firmicutes have been established to inhibit inflammation, which possibly explains the anti-inflammatory effects of LGG.[34] A meta-analysis report revealed that a lower *Bacteroidetes* level is associated with higher incidence of inflammatory bowel disease.[35] This gives an idea of the inflammation regulatory role of *Bacteroidetes*. In LGG treated *Salmonella*-infected mice, *Bacteroidetes* have increased by nearly 2 log. This may explain how LGG could regulate the inflammation in *Salmonella*-infected neonates.

LGG treatment alters the host metabolome

PCA, classification and heat map analysis (Fig. 5) revealed that *Salmonella* infected and LGG treated mice clustered differently and altered metabolite profiling. Further analyses suggested that the downregulated metabolites following challenge compared to the untreated control could reveal some meaningful biological pathways while no pathways could be identified from the list of upregulated metabolites in either LGG treated or LGG treated but ST challenged mice. In both LGG treated and *Salmonella* infected LGG treated mice, purine metabolism and nicotinate and nicotinamide metabolism were downregulated (Fig. 6A and B).

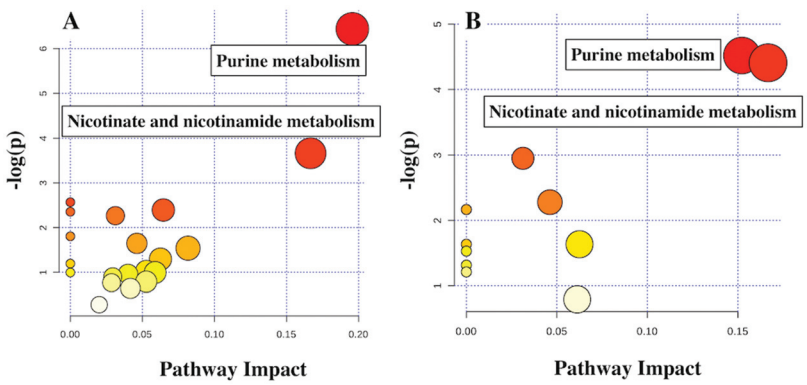

Fig. 6 LGG treatment downregulates purine, nicotinate and nicotinamide metabolism pathways. A: Pathway analysis for downregulated metabolites in LGG treated day 8 pi in blood serum of neonates. B: Pathway analysis for downregulated metabolites in *Salmonella* challenged LGG treated day 8 pi in blood serum of neonates. Because of low volume, serum from 6 neonatal mice per treatment condition was pooled and the results presented are the average of 3 such pools (each of n = 6) per condition.

Discussion

The current study is novel because perhaps this is the first report revealing the effect of LGG in protecting neonate mice against *Salmonella* challenge. The only other study in a related area that is available revealed that colonization of LGG in neonatal mice could reduce susceptibility to colitis in adulthood.[8] The current report established for the first time the efficacy and mechanism by which LGG can alleviate *Salmonella* infection in neonate mice. Neutrophil infiltration marks the inflammation of the intestine. Neutrophil phagosome complexes kill pathogens by expressing Myeloperoxidase (MPO), which helps in generating oxygen free radicals. *Salmonella* infection causes massive neutrophil infiltration leading to diarrhea.[36] MPO activity was also significantly decreased as compared to *Salmonella* challenge (Fig. 3B). Studies with IL10 knockout mice showed higher pathogenesis and larger mortality than normal mice, suggesting that IL-10 played an important role in controlling *Salmonella* infection.[7] Reports from gene expression and cytokine level studies showed an increase in IL-10 expression following treatment with LGG (Table 1, Fig. 3D) to promote anti-inflammation.

Salmonella infection destroyed the gut epithelium structure and severely damaged the gut barrier function. ST challenge caused an increase in gut permeability, which led to increased inflammation in the gut.[14] It was reported earlier that treatment with LGG could (a) increase the expression of tight junction proteins, and (b) decrease gut permeability to compromise barrier function.[37] In this report, we established that transcriptional expression levels of the tight junction proteins are present in higher amount in LGG treated pups that were either challenged or not challenged with ST (Fig. 3E–G).

Salmonella mediated infection leads to a stage of multiple organ failure and sepsis which causes fatigue and muscle weakness. This accounts for strength related defects. The behavioural tests such as the grip strength test and the ambulation test showed clearly that *Salmonella*-infected pups are weaker in strength as established in the current report. LGG treatment recovered mice from infection and subsequently from strength related defects (Fig. 4A, C, and D). Defects in lower limb grasping, (Fig. 4B) in *Salmonella*-infected pups are probably due to lower abdominal pain caused by severe gut inflammation following ST challenge. LGG treatment could significantly alleviate the defects.

Loss of gut microbial diversity was associated with inflammation and infectious diseases.[38] Probably the inflammatory burst causes a decrease in microbial diversity in the gut in *Salmonella*-infected mice. LGG treatment was shown to restore the microbiota diversity in *Salmonella*-infected pups, which may be due to the regulated inflammation in the gut (Fig. 5C). The decrease in microbial diversity in mice treated with LGG alone can be explained by Th2 modulation through LGG, which increased mucus, host defence peptide and IgA secretion.

Nicotinate metabolism and nicotinamide metabolism were related to inflammation and, in fact, drugs like Saikosaponins had been reported to inhibit inflammation by regulating this pathway.[39] This study hinted at a possible mechanism by which LGG treatment can regulate the inflammation (Fig. 6A and B). It was also reported that upregulation of purine metabolism led to the production of a large amount of uric acid that can disrupt the gut epithelial barrier and might increase the gut permeability.[40] The current study also revealed an increase in the gut epithelial barrier function upon decreasing gut permeability in LGG treated mice (Fig. 6A and B). Downregulation of purine metabolism can, therefore, be a possible mechanism by which LGG treatment decreases gut permeability. Further studies are needed to establish the detailed mechanism; for example, IL-10 knockout mice can be used to check if the anti-inflammation is through IL-10 secretion. The current study revealed that LGG treatment rescued the pups from *Salmonella* mediated pathogenesis. *Salmonella* infected neonate gut tissue showed higher expression of inflammatory markers in contrast with the *Salmonella* infected pups following treatment with LGG, which showed a reduction in inflammatory markers and an increase in the expression of anti-inflammatory genes. Results from gut histology and MPO revealed that the *Salmonella*-infected gut was severely damaged. Similarly, the junction protein expression was also low in *Salmonella*-infected mice but increased expression was seen following treatment with LGG. Microbiota diversity in the *Salmonella* infected gut was low and can be restored following treatment with LGG.

Conclusions

The current results from our host metabolomic study showed the potential pathways by which LGG treatment may be playing a crucial role in reducing inflammation and increasing gut epithelial barrier function. The current study showed potential functional pathways by which LGG treatment could rescue the neonate mice following *Salmonella* challenge. The current report is novel as it has established the role of an important probiotic in protecting neonates against *Salmonella* infection. *Salmonella* infection in neonates is a global problem that requires a solution. The current study in neonates has the potential to lead to further clinical studies to explore the possibility.

Conflicts of interest

There are no conflicts to declare.

Acknowledgements

We are thankful to Mr Madan Mohan Mallick, a technician at the Institute of Life Sciences, Bhubaneswar, Odisha, India for assistance in preparing the initial histological slides. This research received no specific grant from any funding agency in the public, commercial, or not-for-profit sectors.

References

1 L. Liu, H. L. Johnson, S. Cousens, J. Perin, S. Scott, J. E. Lawn, I. Rudan, H. Campbell, R. Cibulskis, M. Li, C. Mathers and R. E. Black, Global, regional, and national causes of child mortality: an updated systematic analysis for 2010 with time trends since 2000, *Lancet*, 2012, **379**, 2151–2161.

2 J. S. Gunn, J. M. Marshall, S. Baker, S. Dongol, R. C. Charles and E. T. Ryan, Salmonella chronic carriage: epidemiology, diagnosis, and gallbladder persistence, *Trends Microbiol.*, 2014, **22**, 648–655.

3 H.-M. Chen, Y. Wang, L.-H. Su and C.-H. Chiu, Nontyphoid Salmonella Infection: Microbiology, Clinical Features, and Antimicrobial Therapy, *Pediatr. Neonatol.*, 2013, **54**, 147–152.

4 P. Thiennimitr, S. E. Winter, M. G. Winter, M. N. Xavier, V. Tolstikov, D. L. Huseby, T. Sterzenbach, R. M. Tsolis, J. R. Roth and A. J. Baumler, Intestinal inflammation allows Salmonella to use ethanolamine to compete with the microbiota, *Proc. Natl. Acad. Sci. U. S. A.*, 2011, **108**, 17480–17485.

5 S. E. Winter, P. Thiennimitr, M. G. Winter, B. P. Butler, D. L. Huseby, R. W. Crawford, J. M. Russell, C. L. Bevins, L. G. Adams, R. M. Tsolis, J. R. Roth and A. J. Bäumler, Gut inflammation provides a respiratory electron acceptor for Salmonella, *Nature*, 2010, **467**, 426–429.

6 C. Lupp, M. L. Robertson, M. E. Wickham, I. Sekirov, O. L. Champion, E. C. Gaynor and B. B. Finlay, Host-Mediated Inflammation Disrupts the Intestinal Microbiota and Promotes the Overgrowth of Enterobacteriaceae, *Cell Host Microbe*, 2007, **2**, 119–129.

7 B. Stecher, R. Robbiani, A. W. Walker, A. M. Westendorf, M. Barthel, M. Kremer, S. Chaffron, A. J. Macpherson, J. Buer, J. Parkhill, G. Dougan, C. von Mering and W.-D. Hardt, *Salmonella enterica* Serovar Typhimurium Exploits Inflammation to Compete with the Intestinal Microbiota, *PLoS Biol.*, 2007, **5**, e244.

8 F. Yan, L. Liu, H. Cao, D. J. Moore, M. K. Washington, B. Wang, R. M. Peek, S. A. Acra and D. B. Polk, Neonatal colonization of mice with LGG promotes intestinal development and decreases susceptibility to colitis in adulthood, *Mucosal Immunol.*, 2016, **10**, 117–127.

9 T. Pessi, Y. Sutas, M. Hurme and E. Isolauri, Interleukin-10 generation in atopic children following oral *Lactobacillus rhamnosus* GG, *Clin. Exp. Allergy*, 2000, **30**, 1804–1808.

10 T. S. Wallis and E. E. Galyov, Molecular basis of Salmonella-induced enteritis, *Mol. Microbiol.*, 2000, **36**, 997–1005.

11 R. L. Santos, S. Zhang, R. M. Tsolis, R. A. Kingsley, L. G. Adams and A. J. Baumler, Animal models of Salmonella infections: enteritis versus typhoid fever, *Microbes Infect.*, 2001, **3**, 1335–1344.

12 M. Barthel, S. Hapfelmeier, L. Quintanilla-Martinez, M. Kremer, M. Rohde, M. Hogardt, K. Pfeffer, H. Russmann and W. D. Hardt, Pretreatment of mice with streptomycin provides a *Salmonella enterica* serovar Typhimurium colitis model that allows analysis of both pathogen and host, *Infect. Immun.*, 2003, **71**, 2839–2858.

13 T. D. Lawley, D. M. Bouley, Y. E. Hoy, C. Gerke, D. A. Relman and D. M. Monack, Host transmission of *Salmonella enterica* serovar Typhimurium is controlled by virulence factors and indigenous intestinal microbiota, *Infect. Immun.*, 2008, **76**, 403–416.

14 K. Zhang, A. Dupont, N. Torow, F. Gohde, S. Leschner, S. Lienenklaus, S. Weiss, M. M. Brinkmann, M. Kuhnel, M. Hensel, M. Fulde and M. W. Hornef, Age-dependent enterocyte invasion and microcolony formation by Salmonella, *PLoS Pathog.*, 2014, **10**, e1004385.

15 J. J. Kim, M. S. Shajib, M. M. Manocha and W. I. Khan, Investigating intestinal inflammation in DSS-induced model of IBD, *J. Visualized Exp.*, 2012, (60), pii: 3678.

16 J. Ye, G. Coulouris, I. Zaretskaya, I. Cutcutache, S. Rozen and T. L. Madden, Primer-BLAST: a tool to design target-specific primers for polymerase chain reaction, *BMC Bioinf.*, 2012, **13**, 134.

17 K. D. Pruitt, T. Tatusova and D. R. Maglott, NCBI reference sequences (RefSeq): a curated non-redundant sequence database of genomes, transcripts and proteins, *Nucleic Acids Res.*, 2007, **35**, D61–D65.

18 M. Johnson, I. Zaretskaya, Y. Raytselis, Y. Merezhuk, S. McGinnis and T. L. Madden, NCBI BLAST: a better web interface, *Nucleic Acids Res.*, 2008, **36**, W5–W9.

19 R. C. Edgar, MUSCLE: multiple sequence alignment with high accuracy and high throughput, *Nucleic Acids Res.*, 2004, **32**, 1792–1797.

20 B. Pradhan, D. Guha, A. K. Naik, A. Banerjee, S. Tambat, S. Chawla, S. Senapati and P. Aich, Probiotics L. acidophilus and B. clausii Modulate Gut Microbiota in Th1- and Th2-Biased Mice to Ameliorate Salmonella Typhimurium-Induced Diarrhea, *Probiotics Antimicrob. Proteins*, 2018, DOI: 10.1007/s12602-018-9436-5.

21 D. N. Feather-Schussler and T. S. Ferguson, A Battery of Motor Tests in a Neonatal Mouse Model of Cerebral Palsy, *J. Visualized Exp.*, 2016, (117), DOI: 10.3791/53569.

22 J. Xia and D. S. Wishart, Web-based inference of biological patterns, functions and pathways from metabolomic data using MetaboAnalyst, *Nat. Protoc.*, 2011, **6**, 743–760.

23 J. Xia, I. V. Sinelnikov, B. Han and D. S. Wishart, MetaboAnalyst 3.0–making metabolomics more meaningful, *Nucleic Acids Res.*, 2015, **43**, W251–W257.

24 J. G. Caporaso, J. Kuczynski, J. Stombaugh, K. Bittinger, F. D. Bushman, E. K. Costello, N. Fierer, A. G. Pena, J. K. Goodrich, J. I. Gordon, G. A. Huttley, S. T. Kelley, D. Knights, J. E. Koenig, R. E. Ley, C. A. Lozupone, D. McDonald, B. D. Muegge, M. Pirrung, J. Reeder, J. R. Sevinsky, P. J. Turnbaugh, W. A. Walters, J. Widmann, T. Yatsunenko, J. Zaneveld and R. Knight, QIIME allows analysis of high-throughput community sequencing data, *Nat. Methods*, 2010, **7**, 335–336.

25 T. Z. DeSantis, P. Hugenholtz, N. Larsen, M. Rojas, E. L. Brodie, K. Keller, T. Huber, D. Dalevi, P. Hu and

G. L. Andersen, Greengenes, a chimera-checked 16S rRNA gene database and workbench compatible with ARB, *Appl. Environ. Microbiol.*, 2006, **72**, 5069–5072.

26 T. Z. DeSantis Jr., P. Hugenholtz, K. Keller, E. L. Brodie, N. Larsen, Y. M. Piceno, R. Phan and G. L. Andersen, NAST: a multiple sequence alignment server for comparative analysis of 16S rRNA genes, *Nucleic Acids Res.*, 2006, **34**, W394–W399.

27 A. Dhariwal, J. Chong, S. Habib, I. L. King, L. B. Agellon and J. Xia, MicrobiomeAnalyst: a web-based tool for comprehensive statistical, visual and meta-analysis of microbiome data, *Nucleic Acids Res.*, 2017, **45**, W180–W188.

28 M. G. Langille, J. Zaneveld, J. G. Caporaso, D. McDonald, D. Knights, J. A. Reyes, J. C. Clemente, D. E. Burkepile, R. L. Vega Thurber, R. Knight, R. G. Beiko and C. Huttenhower, Predictive functional profiling of microbial communities using 16S rRNA marker gene sequences, *Nat. Biotechnol.*, 2013, **31**, 814–821.

29 C. A. Henard and A. Vazquez-Torres, Nitric oxide and salmonella pathogenesis, *Front. Microbiol.*, 2011, **2**, 84.

30 D. Hersh, D. M. Monack, M. R. Smith, N. Ghori, S. Falkow and A. Zychlinsky, The Salmonella invasin SipB induces macrophage apoptosis by binding to caspase-1, *Proc. Natl. Acad. Sci. U. S. A.*, 1999, **96**, 2396–2401.

31 S. Hapfelmeier, B. Stecher, M. Barthel, M. Kremer, A. J. Muller, M. Heikenwalder, T. Stallmach, M. Hensel, K. Pfeffer, S. Akira and W. D. Hardt, The Salmonella pathogenicity island (SPI)-2 and SPI-1 type III secretion systems allow Salmonella serovar typhimurium to trigger colitis via MyD88-dependent and MyD88-independent mechanisms, *J. Immunol.*, 2005, **174**, 1675–1685.

32 A. Vazquez-Torres, B. A. Vallance, M. A. Bergman, B. B. Finlay, B. T. Cookson, J. Jones-Carson and F. C. Fang, Toll-like receptor 4 dependence of innate and adaptive immunity to Salmonella: importance of the Kupffer cell network, *J. Immunol.*, 2004, **172**, 6202–6208.

33 I. Kastenberger, C. Lutsch, H. Herzog and C. Schwarzer, Influence of sex and genetic background on anxiety-related and stress-induced behaviour of prodynorphin-deficient mice, *PLoS One*, 2012, **7**, e34251.

34 D. N. Frank, A. L. St Amand, R. A. Feldman, E. C. Boedeker, N. Harpaz and N. R. Pace, Molecular-phylogenetic characterization of microbial community imbalances in human inflammatory bowel diseases, *Proc. Natl. Acad. Sci. U. S. A.*, 2007, **104**, 13780–13785.

35 Y. Zhou and F. Zhi, Lower Level of Bacteroides in the Gut Microbiota Is Associated with Inflammatory Bowel Disease: A Meta-Analysis, *BioMed Res. Int.*, 2016, **2016**, 5828959.

36 R. M. Tsolis, L. G. Adams, T. A. Ficht and A. J. Baumler, Contribution of Salmonella typhimurium virulence factors to diarrheal disease in calves, *Infect. Immun.*, 1999, **67**, 4879–4885.

37 R. M. Patel, L. S. Myers, A. R. Kurundkar, A. Maheshwari, A. Nusrat and P. W. Lin, Probiotic bacteria induce maturation of intestinal claudin 3 expression and barrier function, *Am. J. Pathol.*, 2012, **180**, 626–635.

38 J. Y. Chang, D. A. Antonopoulos, A. Kalra, A. Tonelli, W. T. Khalife, T. M. Schmidt and V. B. Young, Decreased diversity of the fecal Microbiome in recurrent Clostridium difficile-associated diarrhea, *J. Infect. Dis.*, 2008, **197**, 435–438.

39 Y. Ma, Y. Bao, S. Wang, T. Li, X. Chang, G. Yang and X. Meng, Anti-Inflammation Effects and Potential Mechanism of Saikosaponins by Regulating Nicotinate and Nicotinamide Metabolism and Arachidonic Acid Metabolism, *Inflammation*, 2016, **39**, 1453–1461.

40 T. R. Chiaro, R. Soto, W. Zac Stephens, J. L. Kubinak, C. Petersen, L. Gogokhia, R. Bell, J. C. Delgado, J. Cox, W. Voth, J. Brown, D. J. Stillman, R. M. O'Connell, A. E. Tebo and J. L. Round, A member of the gut mycobiota modulates host purine metabolism exacerbating colitis in mice, *Sci. Transl. Med.*, 2017, **9**(380), pii: eaaf9044.

